Tracking and Monitoring Pulsatility of a Portion of Inferior Vena Cava from Ultrasound Imaging in Long Axis

Published version:

DOI:10.1016/j.ultrasmedbio.2018.10.024

(Article begins on next page)

Tracking and Monitoring Pulsatility of a Portion of Inferior Vena Cava from Ultrasound Imaging in Long Axis

Luca Mesin[a,*], Paolo Pasquero[b], Silvestro Roatta[c]

[a] *Mathematical Biology and Physiology, Department of Electronics and Telecommunications, Politecnico di Torino, Torino, Italy*
[b] *Department of Medical Sciences, University of Torino, Torino, Italy*
[c] *Integrative Physiology Lab, Department of Neuroscience, University of Torino, Torino, Italy*

Abstract

Pulsatility of the inferior vena cava (IVC) provides information on the volume status in healthy subjects and in many clinical conditions. The ultrasound (US) approach to estimate the caval index (CI) is not standardized, as it is operator-dependent and prone to measurement errors due to different factors, including movements of the IVC and non-uniform IVC pulsatility along its longitudinal axis. We propose and test in healthy subjects an innovative automated approach, which tracks the IVC movements registered in a B-mode US video-clip and estimates the pulsatility of an entire portion of the vein rather than of a single arbitrary section. Large variations of CI estimations were found along the longitudinal axis (in the worst case, CI ranged between 15% and 60%), indicating the importance of investigating a whole portion of the vessel.

*Corresponding Author: Luca Mesin, Dipartimento di Elettronica e Telecomunicazioni, Politecnico di Torino, Corso Duca degli Abruzzi, 24 - 10129 Torino - Italy; Email, luca.mesin@polito.it; Phone, +39 011.090.4085

Keywords: Inferior vena cava, Ultrasound, Tracking, Caval index

Introduction

A non-invasive, widely adopted method to assess the intravascular volume status is based on the pulsatility of the diameter of the inferior vena cava (IVC), estimated from ultrasound (US) measurements. It found applications in both healthy subjects (Pasquero et al. (2015)) and conditions of altered volemic status in patients (Lichtenstein (2005)). However, standardization of the measurement technique is still lacking (Wallace et al. (2010)). Different recommendations have been proposed on where to measure the vein diameter along a longitudinal section (Wallace et al. (2010), Resnick et al. (2011)). However, the pulsatility of the IVC along its longitudinal axis may not be homogeneous (Mesin et al. (2015)). As a result, diagnostic recommendations are non-uniform (Zhang et al. (2014)).

Pulsatility is measured in terms of the caval index (CI), reflecting the variations of vessel diameter during the respiratory cycle (Blehar et al. (2012)). However, during respiration, the vessel moves relative to the transducer, inducing an additional source of variability in the assessment of pulsatility. For instance, the M-mode technique allows to monitor changes in IVC diameter along a fixed line, which is actually fixed with respect to the probe, but may fluctuate with respect to the vessel, depending on respiratory movements (Mesin et al. (2015)). Correspondingly, large movement artefacts are produced, particularly if the vein has an irregular shape (Lichtenstein (2005)) or if it rotates.

In a recent paper (Mesin et al. (2015)), we proposed a method for tracking IVC movements in long-axis US scans and estimating its diameter in each frame, along a direction moving together with the vein. This approach has a low computational cost and provides a more reliable estimation of IVC local pulsatility than the standard method (Mesin et al. (2015)). However, the pulsatility along a single section may be not representative of the dynamics of the whole IVC. For example, some parts of the vein can show low pulsations for being anchored to nearby structures (e.g., the diaphragm or vein inlets) (Wallace et al. (2010)).

The non-homogeneous pulsatility of the vessel and the lack of consensus on an optimal measuring site (Wallace et al. (2010), Resnick et al. (2011)) are likely to contribute to the contradicting indications found in the literature (Weekes et al. (2012)). However, investigations on the pulsatile behavior of the IVC at different longitudinal sites have seldom being reported and were never based on simultaneous monitoring of a whole IVC segment because of lack of the necessary computational tools. Here, we propose a new algorithm that tracks the movements and simultaneously monitors the diameter of different sections of a whole portion of the IVC.

Materials and Methods

An algorithm (implemented in MATLAB R2018a, The Mathworks, Natick, Massachusetts, USA) was developed to process each frame of an US B-mode video-clip of a longitudinal view of the IVC. Continuous measurements of the diameters along a whole portion of the IVC were computed after compensating for possible IVC movements.

At the first frame of the clip, the user is asked to provide the following information used by the software for further processing (Figure 1).

1. A rectangular portion including a longitudinal view of the IVC is se-

lected.

2. On this sub-image, the user selects two reference points, assumed as anchoring sites for the vein. The two reference points are connected by a reference segment. The reference point on the left is usually close to the confluence of the hepatic veins into the IVC, the right one is near the lower hepatic region (caudate lobe) or at the confluence between the IVC and the portal vein.

3. The user then draws the leftmost and rightmost segments cutting the IVC transversally, along which the first and last diameter measurements are computed (in Figure 1, they are a few mm proximal to the confluence of the hepatic vein and close to the lower region of caudate lobe, respectively). The user is then asked to select two points close to the borders of the IVC along the leftmost section.

The software then draws a number of lines (21 in this paper) uniformly distributed between the leftmost and rightmost borders set by the user. Specifically, the lines are at the same distance from each other and their slopes vary linearly between those of the two lines originally selected by the user. The vein borders are then identified along each of these lines as described in (Mesin et al. (2015)), by detecting sharp changes in the intensity of the US image (which was first processed by a median filter with a square-shaped mask of 9x9 pixels, in order to smooth the image while still preserving edge locations). As more than one point can show a sharp change of intensity along a given section, the one closest to the borders identified in the previous line was considered. For the leftmost line, this method cannot apply: for this reason, the user is asked to select points close to the border in the first frame, as mentioned above; moreover, for the subsequent frames, the borders identified in the previous frame on the first line were used. Once the superior and inferior IVC borders have been estimated along all intersecting lines, their profiles were further adjusted by a longitudinal smoothing, which compensates for minor estimation errors (e.g., noise in the US image, US artefacts such as reverberation and shadowing). Specifically, for each line, the border position was re-calculated as the mean between its original value and the linear interpolation with its two nearest neighbours.

The movements of the vein were tracked assuming that they were smooth in subsequent frames. Moreover, small linear deformations were considered. The position of each reference point was automatically re-mapped in subsequent frames. An estimation of the displacement exhibited by a reference point from one frame to the next was obtained from the comparison of image portions (size 128x128 pixels) centred on the current position of the reference point in the first frame of the pair. The two portions were aligned in the 2D Fourier domain, to improve resolution (Mesin et al. (2015)). The same method as in (Mesin et al. (2015)) was considered, but the image portion to be aligned was decomposed into 5 sub-regions. The translations of all regions were computed and their mean translation and rotation were estimated. Moreover, from the third frame on, three images were considered (the present one and the two previous frames): the movements from each pair of images were computed imposing that the displacement between the first and the last was the sum of the two displacements from the first to the second and from the second to the third. This procedure was found to provide smoother and more stable movements tracking than using only pairs of subsequent frames.

Given the new positions of the reference points, a new reference segment was calculated, which could appear translated, rotated or stretched compared to the previous frame. On this basis, each line along which to estimate the IVC section was re-calculated by keeping constant the angle of intersection as well as the ratio of the distances between the intersection point and the two reference points. In this way, these lines followed movements and deformations of the IVC and, ideally, always intersected the IVC along the same cross-sections.

The superior and inferior borders of the IVC along each line and for each frame obtained as detailed above were affected by high frequency and quantization noises. To improve them, the time series (representing the position of each point of the borders over time) were low pass filtered with a cut-off frequency of 4 Hz (this filter and the ones mentioned below were of Butterworth type, order 4 and used twice, once with time reversed, to remove phase distortion and delay).

Then, the vessel midline was computed as the average between the two borders. It was then approximated by a polynomial function of order 4 (hereinafter, the term IVC midline indicates this polynomial approximation). Then, 10 points were uniformly distributed along the midline of the vein, excluding the first and last 5% of the curve, to avoid possible edge effects. Then, the sections orthogonal to the IVC midline passing from each such points were considered. The IVC diameters in these sections were computed by interpolation from the estimated vein borders (sampled on the 21 sections considered by the software). Specifically, the two samples of the considered border closest to the line orthogonal to the IVC midline were identified; then, the line passing through these two samples was computed; the intersection point between such a line and the one orthogonal to the IVC midline was then found. Notice that, in this way, the direction along which to compute the IVC sections was standardized as suggested in (Pasquero et al. (2015)). These ten diameters were further considered in the following.

In each IVC section, pulsatility was quantified by the CI, defined as the ratio between the range of the estimated diameter time series and its maximum (Mesin et al. (2015)). CI values were computed from each respiration cycle (identified based on the low frequency oscillations of the diameter time series appearing after low pass filtering at 0.4 Hz) and their values were averaged obtaining a single index of pulsatility for each section. From these estimates, different indexes could be computed to characterize the overall pulsatility: the mean pulsatility defined as the mean of the CIs in the different longitudinal sections; the maximum CI, which could indicate possible collapse of the vein; the standard deviation of the CIs, indicating the variability of the dynamics along the longitudinal axis.

The method was tested on the same data as (Mesin et al. (2015)) (to which the reader is invited to refer for the details), i.e., on four healthy subjects in supine position during quiet normal breathing (investigated following the tenets of the Declaration of Helsinki). Additional tests are shown in the Supplementary Material. Pulsatility was measured in terms of the CI of each of the 10 sections orthogonal to the longitudinal axis mentioned above. The distribution of these CI estimates was then shown in boxplots, showing median, quartiles and range.

Results

Figure 1 shows the data provided by the user (location of the vein, reference points and left/right range of interest) and the procedure employed by the algorithm to process each frame.

Figure 2 shows an example of processing of data from a subject with an IVC with an irregular profile. The displacement of the vein and the time series of the diameters (measured at different locations along the IVC axis) are shown in 2A and 2B, respectively. Notice the large variability of section sizes along the axis of the vein. Two frames corresponding to local minimum and maximum of average section of the vein are shown in 2C and 2D, respectively.

Figure 3 shows the results of the processing of the video-clips from the four subjects. The pulsatility was estimated in terms of CI, which was computed for each of the 10 sections considered. The boxplot in 3A shows, for each of the four subjects, the distribution of the CI values. Notice that the distributions are very different across subjects. Specifically, subject 4 shows the minimum variations of CI along the axis, with a range of about 19-26%; on the other hand, subject 3 shows the maximum variation of CI along the axis, with values ranging between 15-60%. Minimum and maximum IVC size is shown for these two subjects in Figure 3B. Notice that subject 4 has an IVC with about constant section that indeed pulsates uniformly, whereas the vein of subject 3 shows low and high pulsatility at proximal (left) and distal (right) IVC sites, respectively.

Discussion

The need of exploring an entire portion of IVC

Diameter oscillations of the IVC are not always homogeneously exhibited in the tract of the vein observed in longitudinal scans, especially in the case of non-uniform appearance. For example, the retrohepatic IVC may be anchored to other structures, like the diaphragm or hepatic vein inlet with a consequent irregular collapse. Two subjects out of the four considered here showed large variations of pulsatility in the different sections (subjects 2 and 3, Figure 3). Additional tests are shown in the Supplementary Material, where other 10 healthy subjects are investigated. Most of them show large variations of IVC pulsatility in different longitudinal sections.

This paper proposes a method to investigate automatically the pulsatility of the IVC in an entire portion along the longitudinal course of the vein. The algorithm is an extension of the method proposed in (Mesin et al. (2015)), which describes the tracking of the vein for the assessment of CI along a single IVC section. As compared to the standard CI assessment, based on US scans in M-mode configuration, IVC tracking proved to considerably reduce artefacts due to the displacements of the vein in connection with movements of the diaphragm (Mesin et al. (2015)). In addition to vein tracking, the novel algorithm allows to compute IVC borders in a region of interest, which can span several centimetres, depending on the subject's echogenicity. By a post-processing, it is also possible to estimate the pulsatility along an optimal direction, i.e., orthogonal to the midline of the vessel (Pasquero et al. (2015)). On the other hand, with the standard M-mode approach, the direction of the M-line is constrained to originate from the probe and may thus intersect the IVC along a sub-optimal direction. Notice also that, by using the single diameter studied in (Mesin et al. (2015)), it is not easy for the operator to select a line orthogonal to the midline, whereas it is simple to compute it automatically once the IVC borders are available on an entire portion of the vein along the longitudinal direction. Finally, the possibility to simultaneously collect and average the CI from the different sections along the displayed IVC segment reduces the uncertainty related to the arbitrary choice of a given single section, as done in standard CI assessments.

Perspectives

The proposed algorithm opens new perspectives in the study of IVC pulsatility. For instance it makes possible to investigate whether the IVC exhibits systematic changes in pulsatility along the longitudinal axis. In addition, a global CI can be conceived, as the average of the CIs obtained in the different IVC sections, which may possibly yield a more objective and repeatable estimation of IVC pulsatility than the standard approach. This issue is currently under investigation and preliminary results support the hypothesis (Mesin et al., unpublished observations on 10 healthy subjects investigated twice by three operators). Further analysis of the multi-section IVC monitoring may also include the distinct assessment of the respiratory and cardiac oscillatory components (extracted by filtering the diameter time series on specific bandwidths). While the latter has already been the object of some investigation (Folino et al. (2017), Nakamura et al. (2013)), the respiratory component has not previously been studied. Moreover, the global CI was found to be correlated with the right atrial pressure and useful for its non-invasive estimation, on the contrary of the standard pulsatility estimations (Mesin et al., unpublished observations on about 50 patients undergoing right heart catheterization for measuring the atrial pressure). Finally, recent works in progress indicate that there is a good correlation of the average CI (as an overall pulsatility index) with the volemic status of patients (preliminary study on 64 patients either hypo-, eu- or hyper-volemic).

Limitations and possible future improvements

The algorithm is not fully automated, as a few interactions with the user are required to run the processing. In particular, the small area containing the vein needs to be indicated. This preliminary step could be removed by including a method able to identify the IVC automatically (Chen et al. (2018)).

Moreover, the user has to indicate two reference points, which should be easily tracked. Automated detection of points with maximal discrimination and invariant under different transformations could be obtained considering standard image matching techniques, e.g., based on Harris detector, scale invariant feature transform (SIFT) or speed up robust feature (SURF) (Riha et al. (2018)). An alternative could be using the popular speckle noise tracking to estimate the full motion of the vessel (Krupa et al. (2007)).

The present semi-automated implementation opens the problem of assessing the repeatability of the results when the software is run many times, with different inputs. A general assessment is not possible, as the output depends on the specific video-clip and on the actual portion of vein which is selected by the user. However, as a preliminary test, the same video-clip (i.e., the one recorded from subject 3, showing the largest variations) was processed 8 times, considering different selections of input data. The estimated distributions of CI were very similar. Indeed, the following parameters were extracted from them (given in terms of mean $\pm$ standard deviation): mean 0.416 ± 0.027, median 0.447 ± 0.028, standard deviation 0.168 ± 0.013, range 0.454 ± 0.033.

A more important limitation is related to the separation between the US recording and the off-line processing. This introduces a delay in the assessment and also it does not provide immediate feedback about whether the quality of the US imaging is adequate for the processing. This problem could be solved by a real time algorithm embedded into the US system, which would provide the rendering of the estimated IVC borders, guiding the operators in the acquisition of optimal video-clips. The embedding of the software in a US machine requires to reduce the computational time. The present implementation (sequential, interpreted code, implemented in MATLAB R2018a), when run on an average personal computer (with Intel(R) Core(TM) i7-7500U, Double-Core, clock frequency of 2.9 GHz, 8 GB of RAM and 64 bits operating system), took about 400 ms per frame (i.e., about 2 minutes to process a video-clip of 300 frames as those considered here). The processing time could be largely reduced by considering a compiled implementation embedded on a US machine with a powerful processor (a parallel implementation on a GPU or an FPGA could also be considered). Notice also that the frequency range of the investigated signal is of a few Hz, so that the video-clip could be sampled with a frame rate of about 10 Hz, reducing further the computational cost.

Conclusions

We introduced an algorithm to track the movements and identify the borders of an entire portion of IVC in long axis US scans. The proposed method helps to 1) reduce movement artefacts, 2) improve objectivity in the assessment of IVC pulsatility (as the arbitrary choice of a single IVC section is eliminated as well as the choice of the respiratory cycle, as different sections are automatically studied and all breath cycles are identified and the IVC pulsatility is averaged across them), 3) improve stability and accuracy of the estimation by measuring perpendicularly to the vessel axis.

Simultaneous monitoring of several sections of a whole IVC segment significantly extends current US capabilities, providing a longitudinal description of IVC size and pulsatility and revealing possibly relevant regional differences in its elastic behavior.

An instrument implementing the algorithm described in this paper was recently patented by Politecnico di Torino and Universitá di Torino (patent number 102017000006088).

References

Blehar D, Resop D, Chin B, Dayno M, Gaspari R. Inferior vena cava displacement during respirophasic ultrasound imaging. Critical Ultrasound Journal, 2012;4:1–5.

Chen J, Li J, Ding X, Chang C, Wang X, Ta D. Automated identification and localization of the inferior vena cava using ultrasound: An animal study. Ultrason Imaging, 2018;40:232–244.

Folino A, Benzo M, Pasquero P, Laguzzi A, Mesin L, Messere A, Porta M. Roatta S. Vena cava responsiveness to controlled isovolumetric respiratory efforts. Journal of Ultrasound in Medicine, 2017;36:2113–2123.

Krupa A, Fichtinger G, Hager G. Full motion tracking in ultrasound using image speckle information and visual servoin. Proc. ICRA, 2007:2458–2464.

Lichtenstein D. Inferior vena cava. general ultrasound in the critically ill. Berlin: Springer, 2005;23:82.

Mesin L, Pasquero P, Albani S, Porta M, Roatta S. Semi-automated tracking and continuous monitoring of inferior vena cava diameter in simulated and experimental ultrasound imaging. Ultrasound Med Biol, 2015;41:845–857.

Nakamura K, Tomida M, Ando T, Sen K, Inokuchi R, Kobayashi E, Nakajima S, Sakuma I, Yahagi N. Cardiac variation of inferior vena cava: new concept in the evaluation of intravascular blood volume. J Med Ultrasonics, 2013;40:205–209.

Pasquero P, Albani S, Sitia E, Taulaigo A, Borio L, Berchialla P, Castagno F, Porta M. Inferior vena cava diameters and collapsibility index reveal early volume depletion in a blood donor model. Crit Ultrasound J., 2015;7:17.

Resnick J, Cydulka R, Platz E, Jones R. Ultrasound does not detect early blood loss in healthy volunteers donating blood. J Emer Med., 2011;41:270–275.

Riha K, Zukal M, Hlawatsch F. Analysis of carotid artery transverse sections in long ultrasound video sequences. Ultrasound Med Biol., 2018;44:153–167.

Wallace D, Allison M, Stone M. Inferior vena cava percentage collapse during respiration is affected by the sampling location: an ultrasound study in healthy volunteers. Acad Emerg Med, 2010;17:96–99.

Weekes A, Lewis M, Kahler Z, Stader D, Quirke D, Norton H, Almond C, Middleton D, Tayal V. The effect of weight-based volume loading on the inferior vena cava in fasting subjects: a prospective randomized double-blinded trial. Acad Emerg Med., 2012;19:901–907.

Zhang Z, Xu X, Ye S, Xu L. Ultrasonographic measurement of the respiratory variation in the inferior vena cava diameter is predictive of fluid responsiveness in critically ill patients: Systematic review and meta-analysis. Ultrasound Med Biol, 2014;40:845–853.

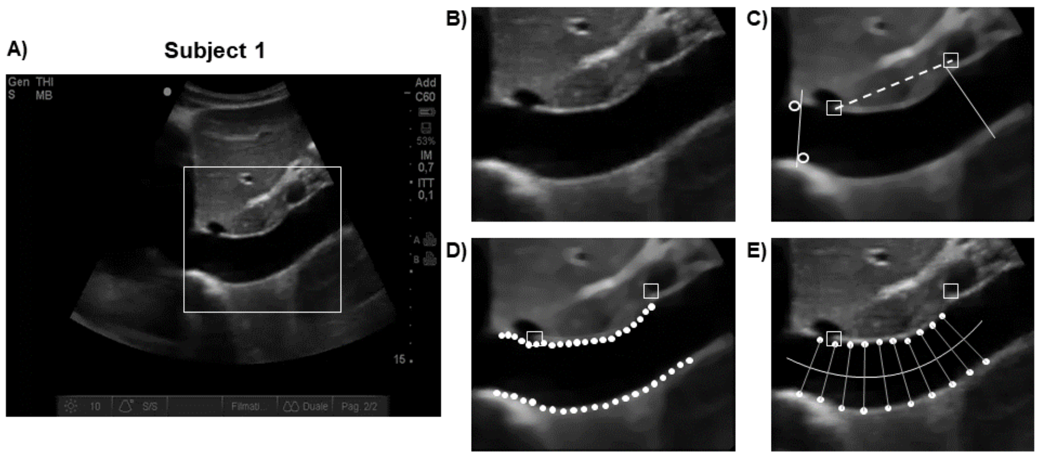

Figure 1: Example of user setting (A-C) and automated processing (D-E) on the first frame of a US video-clip showing a longitudinal view of the IVC. A) Selection of a rectangle including the IVC portion of interest. B) Enlargement of the selected portion, used for further processing. C) Reference points (squares), leftmost and rightmost sections of interest (continuous lines) and points close to the vessel edges along the leftmost section (indicated by circles). Based on these settings, the program defines the reference segment (dashed line) used to track the IVC displacement in subsequent frames. Notice that the image was filtered (by a median filter). D) Automated processing of the algorithm: 21 lines are uniformly distributed between the extreme sections indicated by the user. Along these lines, the profile of the vein is identified (the estimated border points are indicated with small circles). E) Post-processing: from the estimated border of the vessel, the midline is computed and interpolated with a polynomial function of order 4 (curvilinear line); ten equidistant points are selected on this function and new lines perpendicular to it are considered as sections along which the vein diameters are evaluated (border points indicated with small circles).

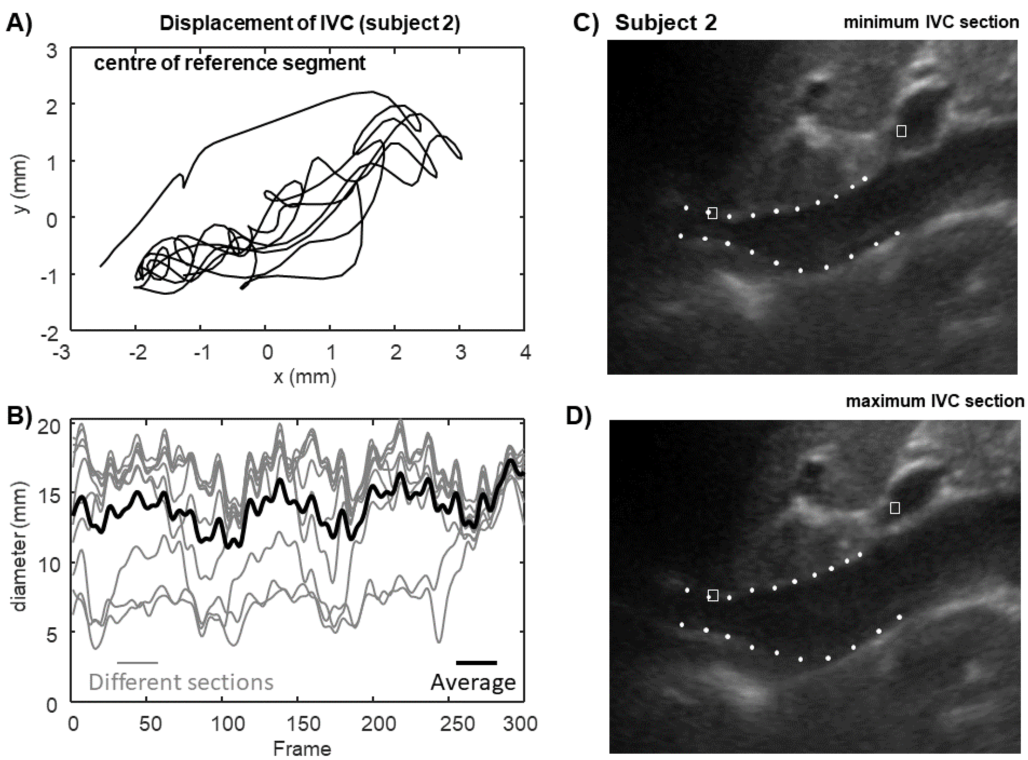

Figure 2: Example of processing of a video-clip. A) Displacement of the IVC shown in terms of the trajectory of the centroid of the reference segment. B) Diameters of 10 sections of the IVC orthogonal to the midline of the vessel (grey lines) and mean value (black line). C) Frame of the video-clip corresponding to a local minimum of the average section. D) Frame of the video-clip corresponding to a local maximum of the average section.

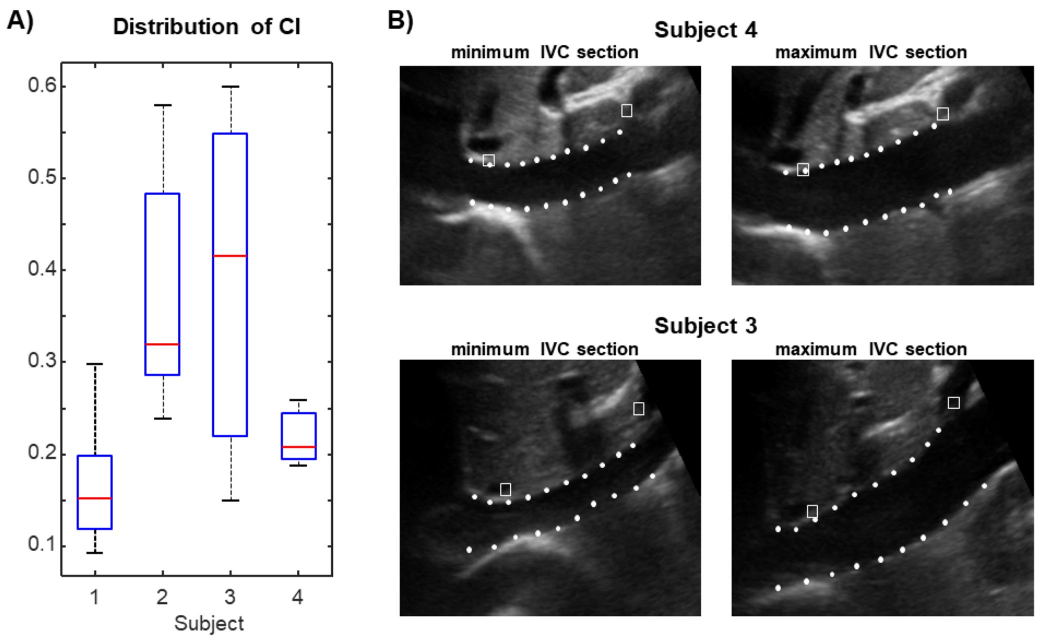

Figure 3: Results of the processing of video-clips from four subjects. A) Distributions of CI along the IVC axis, for each subject (showing median, quartiles and range). B) Two frames of the video-clips of the subjects showing minimum and maximum CI variability (subject 4 and 3, respectively).

SUPPLEMENTARY MATERIAL

Results in addition to those shown in the paper are here presented. Ultrasound (US) data were recorded from other 10 healthy volunteers (5 females, 5 males; age, mean±std 30±13 years, height 172±12 cm, weight 63±11 kg) with a SonoSite M-Turbo system (SonoSite, Bothell, USA; frame rate 30 Hz, resolution about 0.4 mm per pixel, 256 grey levels) equipped with a convex 2-5 MHz probe. Two-dimensional (B-mode) longitudinal views of the inferior vena cava (IVC) were taken with a subxifoideal approach, with the subject in the supine position during relaxed normal breathing. All subjects provided written informed consent for the collection of data and subsequent analysis, according to the Declaration of Helsinki. The experiment was conducted within a study on the repeatability of IVC pulsatility estimation (mentioned in the section Perspectives within the Discussion of the main part of the paper). Different operators repeated twice the acquisition of US video-clips, but only single measurements from a single operator are here considered. The distributions of the caval index (CI) measured along different sections (orthogonal to the estimated axis of the IVC) are shown in Figure 4, for each subject. The CI distributions indicate that there is a large variability among subjects: some of them exhibit little variability of pulsatility along the vessel (like subject number 9) and others have large variations (e.g., subjects 5 has a range of CI of about 25-80% and subject 6 shows a CI range of about 25-95%). These additional results further support the main thesis of the paper: a careful characterization of the dynamics of the IVC requires exploring an entire portion of the vessel, otherwise the assessment of the patient will strongly depend on the specific section considered.

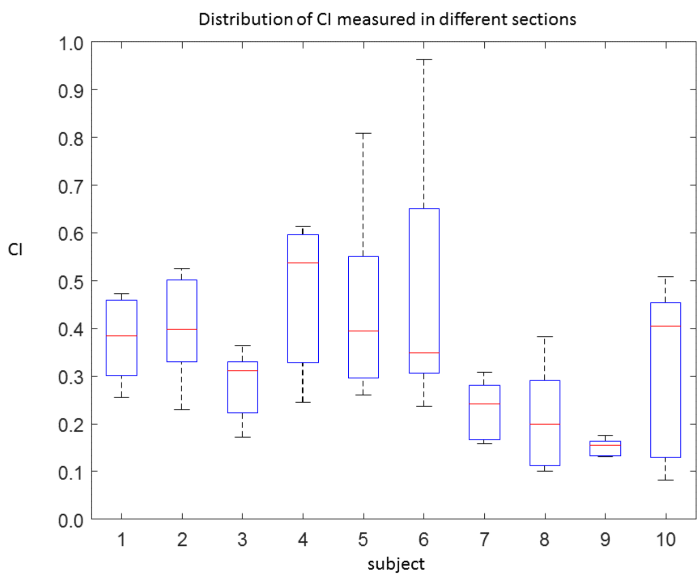

Figure 4: Distribution of CI (median, quartiles and range) considering different longitudinal sections for 10 healthy subjects.